processes

MDPI

Article

Assessing the Effects of Green Surface Coatings on the Corrosion-Related Mechanical Attributes of Materials

Mohammed A. Albadrani

Department of Mechanical Engineering, College of Engineering, Qassim University, Buraydah 51452, Saudi Arabia; moa.albadrani@qu.edu.sa

Abstract

This study investigates the effectiveness of an environmentally friendly coating in mitigating corrosion and preserving the mechanical properties of carbon steel, copper, and aluminium. The coated and uncoated samples were subjected to a 20-day immersion in 5% NaCl solution. Corrosion behaviour was assessed using Linear Sweep Voltammetry (LSV), Open Circuit Potential (OCP), and Electrochemical Impedance Spectroscopy (EIS), while mechanical performance was evaluated through tensile testing. The coating's thickness, surface roughness, water contact angle, and composition were characterised to understand its protective behaviour. The results show that the coating significantly reduced corrosion rates, with carbon steel exhibiting a 99.99% inhibition efficiency and aluminium showing the lowest corrosion rate due to a synergistic effect between the coating and native oxide layer. Mechanical testing revealed that coated carbon steel retained higher tensile strength and stiffness compared to its uncoated counterpart, while aluminium showed notable recovery in elastic modulus. Copper displayed minimal mechanical changes due to its inherent corrosion resistance. This work highlights the potential of eco-friendly coatings in enhancing both the corrosion resistance and mechanical durability of metallic materials in aggressive environments.

Keywords: corrosion; electrochemical; weight loss; environmentally friendly coating; tensile; mechanical properties

check for updates

Academic Editor: Qingmin Yu

Received: 10 July 2025
Revised: 9 August 2025
Accepted: 11 August 2025
Published: 14 August 2025

Citation: Albadrani, M.A. Assessing the Effects of Green Surface Coatings on the Corrosion-Related Mechanical Attributes of Materials. *Processes* **2025**, *13*, 2576. https://doi.org/10.3390/pr13082576

Copyright: © 2025 by the author. Licensee MDPI, Basel, Switzerland. This article is an open access article distributed under the terms and conditions of the Creative Commons Attribution (CC BY) license (https://creativecommons.org/licenses/by/4.0/).

1. Introduction

In this study, "green coatings or eco-coating" refer to environmentally friendly coatings that are designed to reduce environmental impact, such as low-VOC formulations or bio-based coatings. These coatings aim to provide corrosion protection while being sustainable and non-toxic to the environment. This study presents a novel approach by not only investigating the traditional corrosion protection properties of coatings but also linking them to mechanical performance in a comprehensive way. Unlike previous studies, this work provides an in-depth analysis of the synergy between material coatings and mechanical behaviour under corrosive environments, contributing new insights into their long-term sustainability. The selected materials, carbon steel, copper, and aluminium, were chosen based on their widespread industrial use in sectors such as construction, automotives, and electronics. These materials are highly relevant to corrosion protection research, as they are commonly exposed to corrosive environments, and their mechanical properties are critical to structural integrity in these industries.

Recent studies have highlighted bio-based and nanocomposite green coatings as promising corrosion protection strategies [1,2]. Advances in surface science and interface

engineering provide further insight into the roles of surface energy and interface stability in corrosion resistance [3,4].

In this study, the term "eco-friendly coatings" refers to environmentally friendly coatings that are designed to minimise environmental impact, including low-VOC and bio-based formulations. These coatings are applied to protect materials from corrosion while being sustainable and non-toxic. "Industry 4.0" refers to the fourth industrial revolution, characterised by the integration of advanced technologies such as automation, data exchange, and smart manufacturing systems. The relevance of corrosion protection in this context is significant, as these technologies are applied in industries such as construction and automotives, where material integrity is crucial.

Eco-friendly coatings are designed to sustain structural integrity and help to reduce corrosion loss in various industries. Knowledge of the correlation of corrosion resistance to change in mechanical properties is vital in effective long-life performance [4–7]. Copper pipes have long been used in residential water systems because they are durable, whereas the lightweight and corrosion-resistant properties of aluminium are significant factors in Industry 4.0 [2,8–13]. Corrosion in alloys such as steel, aluminium, and copper is aggravated by humidity, pollutants, and electrolytes [2,9–14]. Protective measures such as coating systems, cathodic protection, and corrosion inhibitors have proven effective [3,15–21]. Graphene/α-alumina epoxy coatings, for example, improved dielectric and mechanical properties, while graphene oxide enhanced corrosion inhibition [1,22,23]. Natural inhibitors like *Glycyrrhiza glabra* and imidazole derivatives have also shown high inhibition efficiencies for steel and copper [24,25]. Electrochemical impedance spectroscopy (EIS) is an efficient technique for evaluating charge transfer, diffusion processes, and surface film integrity [2,26]. This study assesses the efficacy of an eco-friendly coating in protecting carbon steel, aluminium, and copper against corrosion and in preserving their mechanical properties after exposure. Coated and uncoated samples (six in total) were immersed in 5% NaCl for 20 days, and corrosion rates, weight loss, and tensile properties were measured. This method provides a complete picture of the relationship between corrosion and the mechanical performance of materials and explores the potential of sustainable coatings to enhance material resilience.

2. Materials and Methods

The corrosion testing methods utilised in this study include Linear Sweep Voltammetry (LSV), Open Circuit Potential (OCP), and Electrochemical Impedance Spectroscopy (EIS). These methods were used to measure corrosion rates, polarisation resistance, and impedance magnitudes, providing a comprehensive understanding of how the coatings improve the material's resistance to corrosion. The results were carefully analysed to correlate corrosion behaviour with mechanical performance, emphasising the significant role of protective coatings in material durability. The following sections detail the methods used in this study, followed by a discussion of the results, which correlate these methods with their respective outcomes in terms of corrosion resistance and mechanical properties.

EIS (Electrochemical Impedance Spectroscopy) is a technique used to measure the impedance of a material to assess its corrosion resistance. The research methodology is described, involving sample preparation, the application of eco-friendly coating, and tests using EIS and potential–dynamic polarisation measurements. Corrosion resistance was determined using the following parameters: electrochemical potential, impedance, polarisation resistance, and corrosion rate. Hardness, tensile strength, Young's modulus, elongation, and impact strength were measured to determine the mechanical properties. The thickness, composition, surface roughness, and the water contact angle of the coating

were also determined. These variables were made to be analysed to figure out how coating properties, corrosion protection, and mechanical performance are related [2,26–29].

2.1. Preparation for the Samples

The thickness of the applied coatings ranged from 50 to 70 microns, depending on the material type and the coating process. The chemical composition of the coating included water-borne acrylic, calcium carbonate, pigments, inorganic fillers, and antimicrobial agents. A 60 µm-thick eco-friendly acrylic coating was applied using a brush-on technique and cured at room temperature for 30 min. The application process was consistent for all samples to ensure uniformity in the coating. A 60 µm-thick water-based acrylic coating containing calcium carbonate, pigments, inorganic fillers, and antimicrobial agents was applied using a brush-on technique. The surface roughness of the coated samples was measured, and the water contact angle was evaluated to assess the coating's ability to resist corrosion. High-purity (95–99.99%) carbon steel, aluminium, and copper samples were used in this study. These materials were prepared according to ASTM D638-14 Type V [27,30]. to ensure uniformity and consistency across all tested samples. The composition of the coating used for coating the samples is well-documented and based on standard formulations for eco-friendly coatings. A detailed analysis of the coating's composition is provided in reference [31], which supports the use of this eco-friendly acrylic coating for corrosion protection. The measured coating thickness was 60 ± 5 µm, the surface roughness (Ra) was 2.3 ± 0.1 µm, the water contact angle was 102° ± 2°, and the composition was as follows: acrylic binder 45 wt%, calcium carbonate 30 wt%, pigments 15 wt%, inorganic fillers 8 wt%, antimicrobial agents 2 wt%. This research is aimed at producing high-purity (95–99.99%) carbon steel, aluminium, and copper samples, prepared according to ASTM D638-14 Type V. Carbon steel contained 1.5% C, 1.3% Mn, 0.5% Si, and the balance Fe. The surface roughness and water contact angle of the coated samples were measured to assess corrosion resistance [2,27], as shown in Figure 1. The samples were coated in an environmentally friendly, water-borne acrylic formula that included calcium carbonate, pigments, inorganic fillers, binders, preservatives, and antimicrobials. The coating did not include phthalates, formaldehyde, heavy metals, solvents, and ultra-low VOC and low odor pigments. Through brush coating, this can be loosely applied, providing the effect of a chalky matte, which can take 30 min. The CS310H device was used to carry out corrosion testing in weight loss mode. The coating was used as an insulating covering; it increases corrosion resistance because it reduces the exposure of the metal surface. The tensile testing was carried out with a Universal Testing Machine (UTM) based on the ASTM [27,30]. Figure 2 contains the eco-friendly coating, the coated samples, and visual durability. This type of coating will have good adhesion and is dependable in corrosion-preventive methods.

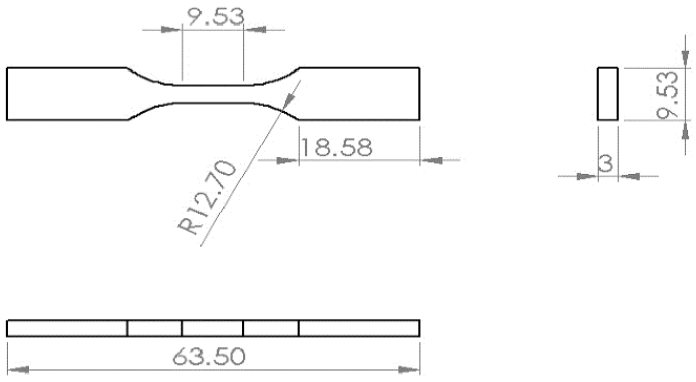


Figure 1. Standard (ASTM D638-14 TYPE V).

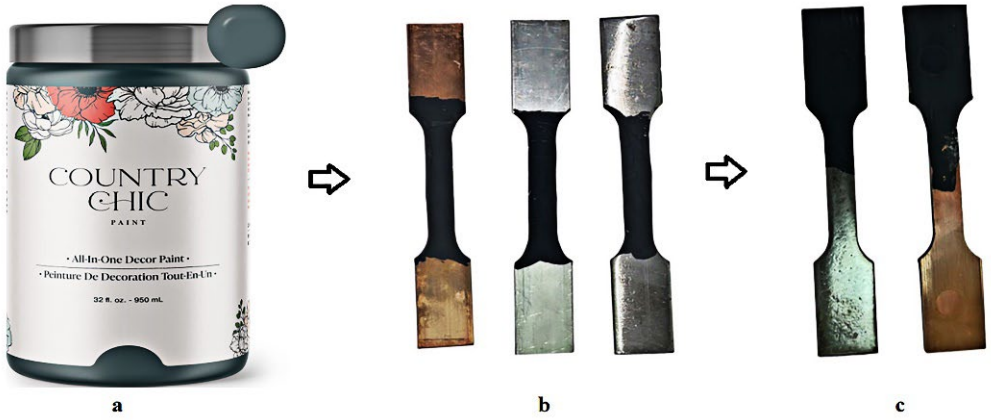


Figure 2. Coating application and sample preparation. (**a**) Eco-friendly coating, (**b**) the samples used in this study, and (**c**) different degrees of durability and resistance to environmental factors and mechanical stress.

2.2. Testing Procedures

To confirm the presence of the coatings on the samples, Scanning Electron Microscopy (SEM) and Energy-Dispersive X-ray Spectroscopy (EDS) were employed. These techniques allowed for the observation of the coating's microstructure and the identification of its elemental composition. Additionally, X-ray Diffraction (XRD) was used to analyse the crystalline structure of the coatings, ensuring their uniformity and effectiveness. Control samples (uncoated materials) were included in the corrosion testing to isolate the effects of the coating. These control samples were subjected to the same environmental conditions and testing methods to serve as a baseline for comparing the efficacy of the coatings. The corrosion testing was performed using a 5% NaCl solution, with samples immersed for 20 days to simulate long-term exposure to corrosive conditions. The test involved the regular monitoring of corrosion rates and mechanical performance, including tensile strength and the modulus of elasticity. This procedure is detailed enough for replication in future studies. The working electrode (WE), reference electrode (RE), and counter electrode (CE) were used in the electrochemical tests to measure corrosion resistance. The RE was a saturated calomel electrode (SCE), and the CE was a platinum electrode. No corrosion inhibitors were used in this study, as the focus was on evaluating the protective effect of the eco-friendly coatings without additional inhibitors. In Equation (3), D represents the diffusion coefficient, which is used to calculate the rate of corrosion based on the electrochemical data collected during testing [29,31–36].

This study used Control System Studio (CSS), an integrated development environment (IDE) (originally created by Texas Instruments to target microcontroller applications) to accomplish the rate of corrosion. The CS310H device was connected to CSS and represents a complete platform to study corrosion, electrochemical research, batteries, environmental chemistry, etc. [26]. In Equation (3), D represents the diffusion coefficient, which is used to calculate the rate of corrosion based on the electrochemical data collected during testing.

The experimental conditions included the infiltration of a specimen into a 5% saline solution consisting of 10 g of salt dissolved into 200 mL of distilled water that was maintained at 24 °C. The system used included three electrodes: the working electrode (WE) was adjacent to the specimen, the reference electrode (RE) was adjacent to the electrolyte solution, and the counter electrode (CE) was closed in circuit. The area of contact between the specimen and solution was 1 cm^2. The aim was to perform degradation testing of materials under corrosive media, and a rate of stretching 10 mm/min was chosen in order to simulate the same conditions.

Numerical simulation was achieved in COMSOL 6.2 Multiphysics, where the filament was assumed to be a viscoelastic fluid with the FENE dumbbell model; meanwhile, fluids were taken to be Newtonian. The most important were the filament diameter (1 mm) and length (10 mm), the velocity of the piston (100 mm/s), the viscosity (0.01 Pa·s), and the density (1000 kg/m^3). The piston velocity was then optimised to generate thinning and break-up characteristics similar to experimental observations.

Electrochemical Impedance Spectroscopy (EIS) was used as a quantifiable technique to evaluate the coating and corrosion resistance. The EIS data inferred such important parameters as impedance magnitude (|Z|), water uptake, and coating resistance through equivalent circuit modelling. Also, Tafel plots were computed using the CSS software CS310H with the help of the non-linear fitting of the Butler–Volmer equation so as to find the corrosion current density, Tafel slopes, polarisation resistance, and corrosion rate. The electrolytic fluid (or the ohmic drop) was adjusted in order to become more accurate. Equivalent Weight (EW) for any chemical element can be determined according to Equation (1). The efficiency of the corrosion inhibitor (IE) and the corrosion rate (CR) were determined by Equations (2) and (3), as follows [1,27–29]:

$$\text{Equivalent Weight } (EW) = \frac{Atomic\ Weight\ of\ element}{Valence\ of\ element\ in\ the\ corrosion\ reaction} \quad (1)$$

$$IE\% = \frac{I_{corr}\ (free) \times I_{corr}\ (inh)}{I_{corr}\ (free)}\ \% \quad (2)$$

$$CR = \frac{I_{corr} \times EW \times 3.27 \times 10^{-3}}{D} \quad (3)$$

2.3. ABAQUS Procedures

In the research, the simulation of a tensile testing of materials and dimensions with the same values as those tested in the experimental study was performed using a finite element method (FEM) study in ANSYS 2023 R2. The simulation was supposed to provide a detailed comparison between a resulting curve of the simulation and the experimental curves of physical testing. An elaborate mesh was developed that would help capture the intricate interactions between the material and the environment when putting it through the tensile test. Realistic boundary conditions were included in order to resemble the testing conditions themselves. The choice of the element size in the mesh was greatly considered to create a compromise between the accuracy of the results and the computational efficiency. The simulation was run on ANSYS software 2023 R2: the meshed geometry was imported, the material properties were assigned to the respective element, the boundary conditions were established, and the solver settings were established. Its outcomes were analysed after post-processing and interpretation where required information was derived. The numerical results and experimental results of the comparison revealed that the simulated curves compared well with the experimental curves. The simulation was practised through a material behaviour model, which detailed the response of materials under loading conditions where the elastic properties and characteristics of plastic deformation were taken into consideration. The rate of stretching was adjusted to fit the experimental conditions to the best degree. The simulation took into consideration the material properties, including Young's modulus, the yield strength, and the ultimate tensile strengths, among others.

3. Results and Discussion

The Finite Element Analysis (FEA) was performed to compare the experimental data with numerical simulations. This analysis allowed for a detailed understanding of how the coatings affected the mechanical performance of the materials under different loading

conditions, providing insights into the material's response to environmental stressors. FEA helped validate the experimental results and offered a deeper understanding of the material behaviour during the corrosion process.

A fracture analysis of the tensile test samples was performed using Scanning Electron Microscopy (SEM). The SEM images revealed important information about the fracture surfaces, indicating the presence of cracks and delamination. The fracture patterns suggested that the coating helped to reduce the propagation of cracks, enhancing the material's toughness and overall mechanical performance. A statistical analysis was incorporated into the study, including error bars on the graphs to reflect the variability in the data. The reproducibility of the results has been assessed through multiple trials, and the data points show consistent trends, confirming the reliability of the experimental findings. The tables have been revised for consistency. Any discrepancies in yield strength values have been corrected, and the tables now reflect accurate and aligned data corresponding to the text.

The observed changes in tensile strength due to corrosion are attributed to the degradation of the coating, which results in the increased exposure of the substrate material to the corrosive medium. This leads to microstructural changes, such as the formation of cracks or pitting, which weaken the material's mechanical properties. Additionally, coating delamination and the onset of microcracks further contribute to the loss of mechanical integrity. Some of the trends observed in the figures appear unusual, particularly in the early stages of corrosion. These anomalies may be attributed to the coating degradation over time, which affects the uniformity of corrosion protection. Further analysis will be needed to understand the underlying mechanisms causing these trends. While the primary driver of mechanical changes is corrosion, other factors such as coating delamination, crack formation, and microstructural changes may also contribute to the observed variations in tensile strength and the modulus. These factors should be considered in future studies for a more comprehensive understanding of material degradation. As indicated in Table 1, the corrosion resistance of the coated samples was significantly improved, with an IE% of 99.992%. This high efficiency was observed in the corrosion tests, demonstrating the effectiveness of the eco-friendly coating in reducing corrosion rates [29,31–36]. In Equation (3), D represents the diffusion coefficient, which is used to calculate the rate of corrosion based on the electrochemical data collected during testing.

Table 1. Comparative Tafel results for carbon steel, copper, and aluminium.

	Sample	Ecorr (mV)	Icorr (μA)	Bc (mV/dec)	Ba (mV/dec)	IE%	CR [mm/year]
Carbon Steel	Uncoated	−0.46483	6.016×10^{-10}	101.58	196.58	0%	4.693×10^{-12}
	Coated	−0.41265	7.5988×10^{-6}	201.67	331.34	99.992%	5.928×10^{-8}
Copper	Uncoated	−0.26258	3.3087×10^{-5}	230.55	110.77	0%	2.589×10^{-7}
	Coated	−0.25757	1.3035×10^{-6}	199.33	218.10	96.06%	1.02×10^{-8}
Aluminium	Uncoated	−1.4847	8.5379×10^{-5}	74.567	598.45	0%	9.306×10^{-7}
	Coated	−0.90329	8.92×10^{-9}	174.99	367.64	99.98%	9.7228×10^{-11}

"Theoretically uncoated" refers to samples that were not subjected to any coating but were treated under the same conditions to compare the impact of coatings on material properties. In this section, the following electrochemical corrosion test results are shown: Linear Sweep Voltammetry (LSV), Open Circuit Potential (OCP), and Electrochemical Impedance Spectroscopy (EIS), along with the post-corrosion mechanical tests of three of the most relevant metallic substrates: carbon steel, copper, and aluminium. The coatings under study were put to test how well they could lower the corrosion current density, enhance the polarisation resistance, and ensure mechanical integrity in isolated saline conditions.

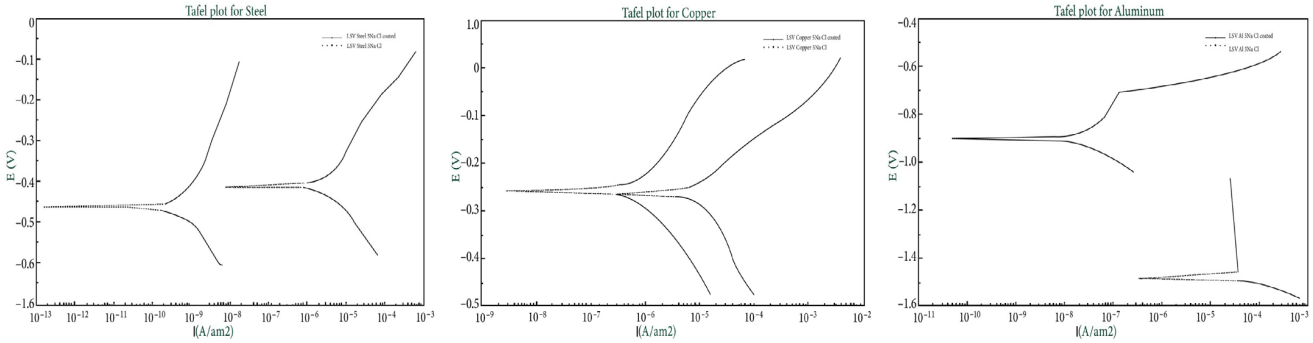
These findings are divided into five main axes of analysis:

- Tafel electrochemical behaviour.
- OCP values yielding a trend towards corrosion potential.
- EIS interfacial parameters.
- Strength and preservation of structure after exposure.
- Relative performance of materials.

All these dimensions helped to develop a more detailed image of how the coating works on the studied substrates.

3.1. Electrochemical Behaviour (Tafel Analysis)

In order to have veritable representation of the corrosion behaviour of the various metals under saline conditions, a Tafel analysis with Linear Sweep Voltammetry (LSV) was used on the carbon steel, copper, and aluminium in coated and theoretically uncoated conditions. Corrosion current density, the correlation direct element of the corrosion rate, was measured and averaged between samples. In the case of carbon steel, as indicated in Figure 3a, Icorr decreased from 7.5988×10^{-6} A/mm^2 (uncoated) to 6.016×10^{-10} A/mm^2 (coated), corresponding to an IE% of 99.992. The CR dropped from 5.928×10^{-8} mm/year to 4.693×10^{-12} mm/year, in accordance with Equation (2); this meant a phenomenal rise in performance. These values are higher than those recorded in the literature, where the rate of corrosion of uncoated carbon steel in the presence of 3.5% NaCl was 5.1×10^{-7} mm/year [28].



(**a**) (**b**) (**c**)

Figure 3. Tafel plots for (**a**) carbon steel, (**b**) copper, and (**c**) aluminium using Linear Sweep Voltammetry (LSV).

In the case of copper, on the other hand, the middle panel of Figure 3b illustrates that the Icorr dropped from 3.3087×10^{-5} A/cm^2 to 1.3035×10^{-6} A/cm^2 (IE % = 96.06). The respective values of CR were 2.589×10^{-7} mm/year and 1.02×10^{-8} mm/year, respectively. These findings verify the efficacy of the coating, yet the contrast between the coated and the uncoated samples is not as dramatic as it is in the case with carbon steel, which is potentially the result of copper possessing higher corrosion resistance on its own.

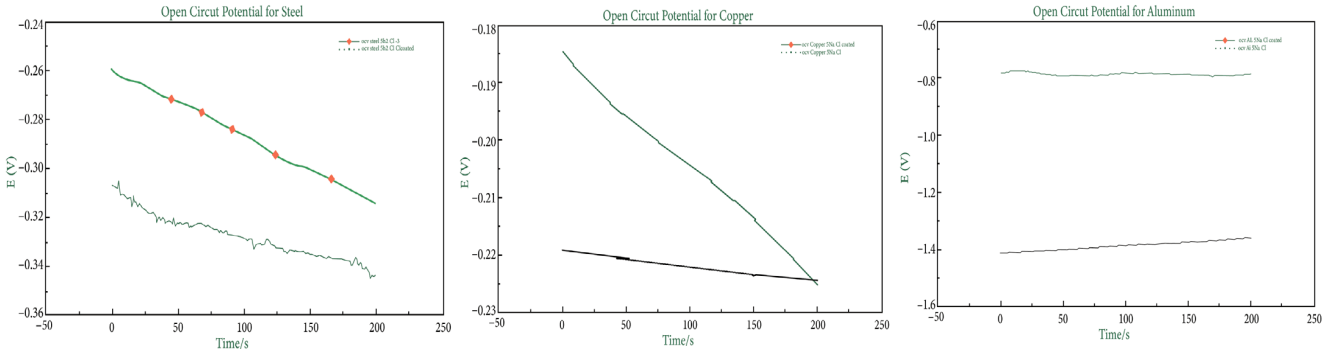
Lastly, as seen in Figure 3c, aluminium recorded the highest % of Icorr, which fell from 8.5379×10^{-5} A/cm^2 to 8.92×10^{-9} A/cm^2 (IE % = 99.98), with the lowest recorded CR of 9.72×10^{-11} mm/year. The coating enhanced the passivity of aluminium despite its high electrochemical activity, and this is probably due to the increased stability of the oxide layers. Surprisingly, the uncoated sample of aluminium also showed a great deal of resistance, mainly due to the formation of the protective oxide film during the testing conditions in a spontaneous manner.

Tafel analysis showed that the carbon steel coating provides near-total protection against corrosion, whereby the rate of corrosion dropped more than 99.99%. Coated aluminium recorded the lowest absolute corrosion rate, implying that there is a synergistic

effect between the coating and the oxide layer on the metal's surface, whereas coated copper recorded moderate improvement, which is attributable to its intrinsic capability of resisting corrosion (see Table 1). One of the main lessons was a much higher resistance of uncoated aluminium, probably because of the presence of passive oxide. In general, this study introduces a coherent evaluation concept of the corrosion behaviour of various metals via LSV, focusing on the fact that Icorr variations, even at the same order of magnitude degree, may substantially affect the performance of these materials.

3.2. Stability of Corrosion Potential (OCP Analysis)

The initial OCP values for the coated samples were generally higher and exhibited less drift over time, indicating effective corrosion protection. Coated aluminium showed the highest electrochemical stability, likely due to synergy between the coating and its native oxide layer. The Open Circuit Potential (OCP) results provided very useful information about the corrosion properties of the metals under testing. In the case of carbon steel (Figure 4a), the uncoated samples experienced a steady decline of 0.26 and 0.31B over 12 h, which means that the corrosion occurred naturally, whereas the coated samples were less vulnerable (a decrease of 0.32 and 0.34B within the same time frame), but with slight oscillations. In the case of copper (Figure 4b), the potential of the uncoated sample assumed a reasonably steady value (−0.22 V), implying acceptable equilibrium and some degree of resistance, whereas that of the coated copper sample showed a much lower OCP (0.8 V) initially, again pointing to a higher protective value, but then slowly decreased, indicating localised coating damage. The uncoated aluminium (Figure 4c) yielded progressively negative values since chloride led to the breakdown of the oxide film, but in the coated sample, the OCP was high (0.8 V) and then fell moderately, indicating great resistance and low activity against the corrosive environment. The outcome notes that in the coated samples, the initial OCP values are higher and the drift with time is lower, indicative of the efficacy of the protective coatings. Interestingly, aluminium coatings exhibited the strongest electrochemical stability, indicating that the protective layer and the rapidly forming native oxide film may be involved in a synergistic process, something that may be taken into consideration in future corrosion-resistant material design.



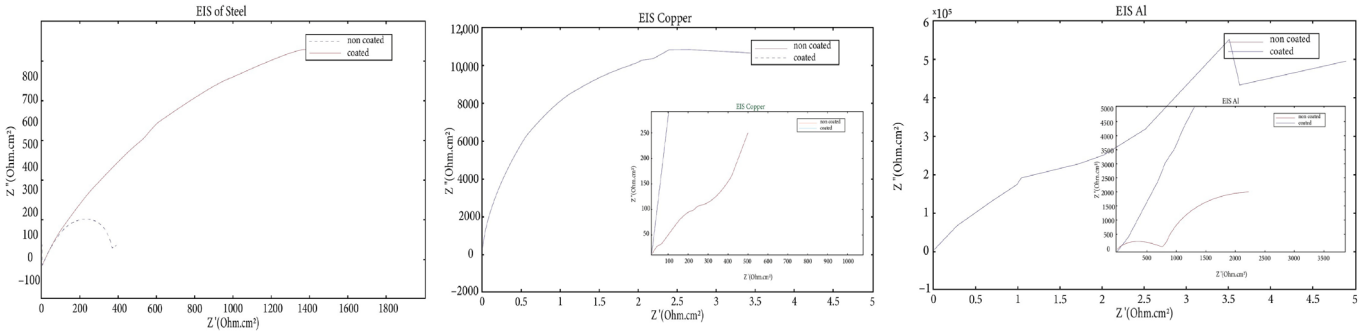
(**a**) (**b**) (**c**)

Figure 4. Open Circuit Potential (OCP) for (**a**) carbon steel, (**b**) copper, and (**c**) aluminium.

3.3. Interfacial Resistance and Capacitance (EIS Analysis)

EIS (Electrochemical Impedance Spectroscopy) is a technique used to measure the impedance of a material to assess its corrosion resistance. In addition to Nyquist plots, Bode plots have been included to provide a more comprehensive view of the corrosion behaviour of the samples. To determine the corrosion resistance of coated and uncoated steel, copper, and aluminium, Electrochemical Impedance Spectroscopy (EIS) was used to determine the corrosion resistance of the specimens in NaCl solutions. There is ample evidence in the

Nyquist plots (Figure 5a–c) that revealed larger arc radii for coated samples, indicating higher impedance. Rp increased from 1638.8 $\Omega \cdot cm^2$ to 2553.6 $\Omega \cdot cm^2$ for coated carbon steel, and from 888.95 $\Omega \cdot cm^2$ to 28 034 $\Omega \cdot cm^2$ for coated copper. The coated aluminium Rp value was higher than the uncoated 804.95 $\Omega \cdot cm^2$. In the case of carbon steel, Figure 5a gave a clear coating effect on the charge transfer resistance (R_{ct}), jumping to 2553.6 compared to 1638.8 $\Omega \cdot cm^2$ of polarisation resistance (Rp). The equivalent circuits proposed indicate that the incorporation of the elements of the coating (Cp, Rp) changes the electrochemical behaviour and gives the effect of a robust barrier. Figure 5b shows a really good boost in copper, where the Rp increased to 28,034 $\Omega \cdot cm^2$ after coating, as portrayed in the circuit diagrams. This reflects the significant restraint of the charge transfer, and this is mainly ascribed to the coating efficacies and the steady interface behaviour represented by the constant phase element (CPE). In the case of aluminium, despite the larger impedance arc presented in Figure 5c in the case of the coated sample, Table 2 indicates an unusual diminution of Rp to 8.079 $\times 10^{-5}$ $\Omega \cdot cm^2$, as compared to 804.95 $\Omega \cdot cm^2$ originally. This can be due to interferences between the deposited coating and the natural but streaming oxide layer, which leads to two time constants in the EIS response and makes the charge mechanism more complicated. In this research, it has been observed that although a coating usually has improved the application against corrosion (as was identified with the help of impedance spectra), their engagement with naturally developing oxide films (especially in the case of aluminium) can decrease their efficiency in the event that they are poorly designed. The difference in Rp among metals brings out that the coating efficiency varies with the type of material, and it should be suggested with surface.



(**a**) (**b**) (**c**)

Figure 5. Electrochemical Impedance Spectroscopy (EIS) for (**a**) carbon steel, (**b**) copper, and (**c**) aluminium.

Table 2. The parameters in the equivalent electrical circuits used to model the electrochemical impedance spectroscopy (EIS) data.

	Steel		**Copper**		**Aluminium**	
	Uncoated	**Coated**	**Uncoated**	**Coated**	**Uncoated**	**Coated**
Rs	17.734	18.472	14.02	16.475	19.71	51.779
Rp	1638.8	2553.6	888.95	28,034	804.95	8.079×10^{-5}
CPE-T	8.5142×10^{-4}	5.4592×10^{-4}	1.8058×10^{-3}	3.98732×10^{-6}	1.7335×10^{-5}	8.5749×10^{-6}
CPE-P	5.4844×10^{-1}	5.9823×10^{-1}	3.8353×10^{-3}	7.7497×10^{-1}	9.07872×10^{-1}	8.1676×10^{-1}

3.4. Mechanical Performance Post-Corrosion Exposure

Tensile tests were conducted on coated and uncoated carbon steel, copper, and aluminium after 20 days of immersion in 5% NaCl solution. This evaluated the effect of corrosion on the metals' mechanical properties. This was performed in order to determine the effectiveness of the protective coating in maintaining the structural integrity of each

material under corrosive pressure. The mechanical parameters, such as tensile strength, Young's modulus, ductility, toughness, and stiffness, were mined and summarised collectively in Table 3, and the stress–strain relationship is depicted in Figure 6a (carbon steel), Figure 6b (copper), and Figure 6c (aluminium).

Table 3. Mechanical properties of carbon steel, copper, and aluminium (coated, uncoated, and reference).

Property	Steel			Copper			Aluminium		
	Uncoated	Coated	Reference	Uncoated	Coated	Reference	Uncoated	Coated	Reference
Max Load (kN)	10.96	11.78	12.26	9.50	9.55	9.48	9.02	8.87	9.21
Max Strength (MPa)	384.39	413.19	430.04	333.37	334.94	332.60	316.39	311.32	323.22
Yield Strength (MPa)	299.35	337.73	338.55	310	318	319	270.86	274.38	278.30
Elastic Modulus E (MPa)	390	400	410	310	270	319	150	280	260
Toughness (kN·mm)	94.64	179.48	186.73	124.31	187.35	186.04	37.02	42.68	56.17
Modulus of Toughness (MPa)	133.74	143.78	258.59	99.40	67.27	67.13	20.46	23.59	31.04
Resilience (kN·mm)	5.39	11.78	10.18	5.80	6.25	6.20	1.65	2.42	2.63
Modulus of Resilience (MPa)	2.98	6.51	5.63	2.03	2.26	2.26	3.04	3.01	3.14
Ductility (Elongation %)	27.21	26.41	26.85	20.61	20.41	20.68	6.97	8.05	10.32
Axial Stiffness (N/mm)	175.04	179.53	184.02	139.13	121.18	143.17	67.32	125.67	116.70

Coating carbon steel proved beneficial. Notably, the ultimate tensile strength (413.19 MPa), yield strength (337.73 MPa), and modulus of elasticity (400 MPa) of the coated specimens increased markedly as compared to the uncoated ones (384.39 MPa, 299.35 MPa, and 390 MPa, respectively). The axial stiffness was improved, as well as the toughness and resilience. These results, as shown in Figure 6a, allay the fact that degradation due to corrosion was successfully alleviated by the coating that assured surface continuity, and the stress concentrations were reduced too. Importantly, the coated steel maintained its mechanical integrity near the reference (uncorroded) specimen, which further supported the effectiveness of the protective coating. The copper, however, had also exhibited stable mechanical results at uncoated and coated conditions, with a minor increase in resilience and toughness in the coated specimens. Table 3 and Figure 6b show that the tensile strength and the yield strength of both the coated and the uncoated samples were almost equal (around 334 MPa and 318 MPa, correspondingly). This adds strength to the natural protection to corrosion exhibited by copper and implies that for short-term strength, coatings seem to have a minimal effect on the overall strength that might be extended by the coatings. The conclusion continues to confirm that the coating is advantageous with regard to long-term durability in harsh saline conditions. Aluminium exhibited unique mechanical behaviour, whereas the relatively good stability of the tensile strength was found in all samples, and a substantial reduction of Young's modulus in approximately 42 per cent of uncoated samples (260 to 150 MPa) was observed. The coated samples, however, recovered to 280 MPa, which shows that the coating prevented corrosion as well as maintained the stiffness of the material. The above alterations, seen in Figure 6c and summarised in Table 3, point to a highly important finding; namely, that the elastic behaviour of aluminium is actually much more susceptible to corrosive wear and tear than its tensile performance may indicate. The fact that this discovery indicates that it is still necessary to explore aluminium's microstructural susceptibility to corrosion.

Tensile tests highlight how coating benefits vary across the three metals. Coated carbon steel recorded the most pronounced mechanical enhancements and coated aluminium surprisingly recorded a very high recovery of the elastic modulus. Being naturally resistant to corrosion, copper experienced slight deviations, and, nonetheless, the coated one was better in terms of resistivity to the elements and the threshold obtained in Red Energy that accrued in this experiment. The results emphasise the need for a thorough mechanical anal-

ysis, besides the tensile strength, to evaluate the effects of corrosion and the effectiveness of coatings on a variety of metallic systems.

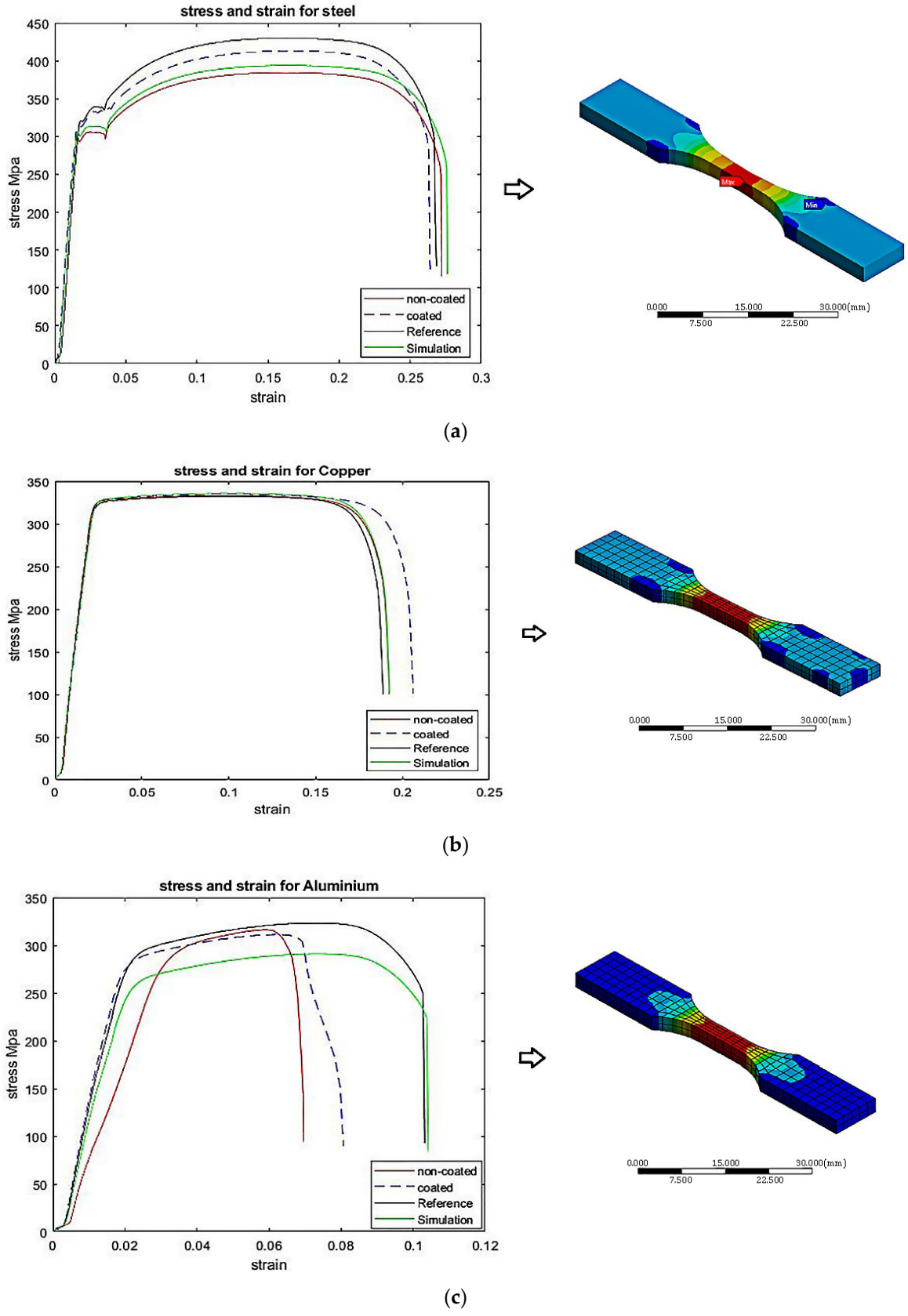


Figure 6. Stress and strain curves for (**a**) steel, (**b**) copper, and (**c**) aluminium with ANSYS simulation.

This paper summarises the electrochemical protection and mechanical toughness of protective coatings applied to three different metals (carbon steel, copper, and aluminium) after exposing them to salt water over a period of 20 days. The trend saw that the coated carbon steel improved a lot in terms of strength and toughness, whereas the coated copper did not change much except that it became slightly better. It was revealed in this work that there is also a stumbling block in the Young tradeoff even though it shows no problem with corrosion resistance, implying that there is minor interaction between the coatings.

4. Conclusions

This research thoroughly evaluated the protective coating dual role in yielding electrochemical corrosion protection as well as the structural durability performance on carbon steel, copper, and aluminium in 5 per cent of salt water after 20 days of immersion. The findings indicated an enormous improvement in all the materials, with aluminium recording the best performance in corrosion protection (a four-order reduction in Icorr value) and coated carbon steel recording the best mechanical properties, such as tensile strength (413.19 MPa) and toughness (179.48 kN·mm). The modestly improved mechanical integrity of coated copper indicated that the same should be expected of aluminium given its superb corrosion resistance but, surprisingly, the Young's modulus declined by more than 42%, indicating either microstructural changes or coating–substrate interactions. These results were also confirmed by Electrochemical Impedance Spectroscopy (EIS), of which coated copper had the biggest impedance arc, and therefore the best surface film quality; these are tabulated in Table 2. The new aspects of this study are the elaboration of a corresponding unified testing approach over metals, an achievement of multi-layer equivalent circuit model validation, and a first report concerning the modulus degradation of aluminium under these conditions, thus providing a wealth of information with regard to coatings in severe, salty environments.

Funding: This research received no external funding.

Data Availability Statement: The original contributions presented in this study are included in the article. Further inquiries can be directed to the corresponding author.

Acknowledgments: The researcher would like to thank the Deanship of Graduate Studies and Scientific Research at Qassim University for financial support (QU-APC-2025).

Conflicts of Interest: The author declares no conflict of interest.

References

1. Zhang, J.; Zhang, W.; Wei, L.; Pu, L.; Liu, J.; Liu, H.; Li, Y.; Fan, J.; Ding, T.; Guo, Z. Alternating multilayer structural epoxy composite coating for corrosion protection of steel. *Macromol. Mater. Eng.* **2019**, *304*, 1900374. [CrossRef]
2. Salim, R.; Ech-chihbi, E.; Fernine, Y.; Koudad, M.; Guo, L.; Berdimurodov, E.; Azam, M.; Rais, Z.; Taleb, M. Inhibition behaviour of new ecological corrosion inhibitors for mild steel, copper and aluminium in acidic environment: Theoretical and experimental investigation. *J. Mol. Liq.* **2024**, *393*, 123579. [CrossRef]
3. Pezzato, L.; Akbarzadeh, S.; Settimi, A.G.; Moschin, E.; Moro, I.; Olivier, M.G.; Brunelli, K.; Dabalà, M. Corrosion and antifouling properties of copper-containing PEO coatings produced on steels. *Surf. Coat. Technol.* **2024**, *482*, 130631. [CrossRef]
4. Jena, G.; George, R.P.; Philip, J. Fabrication of a robust graphene oxide-nano SiO_2-polydimethylsiloxane composite coating on carbon steel for marine applications. *Prog. Org. Coat.* **2021**, *161*, 106462. [CrossRef]
5. Winston, R.R.; Uhlig, H.H. *Corrosion and Corrosion Control: An Introduction to Corrosion Science and Engineering*; Wiley-Interscience: Hoboken, NJ, USA, 2008. [CrossRef]
6. McFarland, M.L.; Provin, T.L.; Boellstorf, D.E. *Drinking Water Problems: Corrosion*; Agrilife Extension: College Station, TX, USA, 2011.
7. Xu, R.; Xin, S.; Ni, Q.; Zeng, H.; Li, M. Initial corrosion characteristics of enamel coated carbon steel in hot tap water. *Russ. J. Electrochem.* **2021**, *57*, 636–643. [CrossRef]

8. Ech-chihbi, E.; Salim, R.; Ouakki, M.; Koudad, M.; Guo, L.; Azam, M.; Benchat, N.; Rais, Z.; Taleb, M. Corrosion resistance assessment of copper, mild steel, and aluminium alloy 2024-T3 in acidic solution by a novel imidazothiazole derivative. *Mater. Today Sustain.* **2023**, *24*, 100524. [CrossRef]
9. Cheng, T.; Huang, H.; Huang, G. Galvanic corrosion behaviour between ADC12 aluminium alloy and copper in 3.5 wt% NaCl solution. *J. Electroanal. Chem.* **2022**, *927*, 116984. [CrossRef]
10. Baena, L.M.; Vásquez, F.A.; Calderón, J.A. Corrosion assessment of metals in bioethanol-gasoline blends using electrochemical impedance spectroscopy. *Heliyon* **2021**, *7*, e07585. [CrossRef]
11. Policastro, S.A.; Anderson, R.M.; Hangarter, C.M. Analysis of galvanic corrosion current between an aluminium alloy and stainless-steel exposed to an equilibrated droplet electrolyte. *J. Electrochem. Soc.* **2021**, *168*, 041507. [CrossRef]
12. Román, A.S.; Méndez, C.M.; Gervasi, C.A.; Rebak, R.B.; Ares, A.E. Corrosion resistance of aluminium-copper alloys with different grain structures. *J. Mater. Eng. Perform.* **2021**, *30*, 131–144. [CrossRef]
13. Jandaghi, M.R.; Saboori, A.; Khalaj, G.; Shiran, M.K.G. Microstructural evolutions and its impact on the corrosion behaviour of explosively welded Al/Cu bimetal. *Metals* **2020**, *10*, 634. [CrossRef]
14. Li, Q.; Zhang, Y.; Cheng, Y.; Zuo, X.; Wang, Y.; Yuan, X.; Huang, H. Effect of temperature on the corrosion behaviour and corrosion resistance of copper–aluminium laminated composite plate. *Materials* **2022**, *15*, 1621. [CrossRef]
15. Xavier, J.R. Galvanic corrosion of copper/titanium in aircraft structures using a cyclic wet/dry corrosion test in marine environment by EIS and SECM techniques. *SN Appl. Sci.* **2020**, *2*, 1341. [CrossRef]
16. Ehsani, A.; Heidari, A.A.; Sajedi, M. Graphene and graphene/polymer composites as the most efficient protective coatings for steel, aluminium and copper in corrosive media: A review of recent studies. *Chem. Rec.* **2020**, *20*, 467–493. [CrossRef] [PubMed]
17. Abubakr, H.M.C.; Ghaith, M.E.; El-Sherif, A.A.; El-Deab, M.S. Influence of metal ions on cysteine as a corrosion inhibitor for low carbon steel in sulfuric acid: Polarisation, EIS, XPS, and DFT analysis. *Int. J. Electrochem. Sci.* **2024**, *19*, 100620. [CrossRef]
18. Wang, N.; Bai, J.Y.; Wen, C.; Li, J.F.; Wang, X.G.; Tong, X.B.; Wang, J. Adaptability of sol-gel anti-corrosion coating on different metallic substrates. *J. Phys. Conf. Ser.* **2021**, *2021*, 012044. [CrossRef]
19. Pezzato, L.; Settimi, A.G.; Fanchin, D.; Moschin, E.; Moro, I.; Dabalà, M. Effect of Cu addition on the corrosion and antifouling properties of PEO coated zinc-aluminised steel. *Materials* **2022**, *15*, 7895. [CrossRef]
20. Ran, Q.; Shi, H.; Meng, H.; Zeng, S.P.; Wan, W.B.; Zhang, W.; Wen, Z.; Lang, X.Y.; Jiang, Q. Aluminium–copper alloy anode materials for high-energy aqueous aluminium batteries. *Nat. Commun.* **2022**, *13*, 576. [CrossRef]
21. El Hawary, M.; Khachani, M.; Benhiba, F.; Kaichouh, G.; Warad, I.; Guenbour, A.; Zarrouk, A.; Bellaouchou, A. Investigation of the corrosion of stainless steel, copper and aluminium in sunflower biodiesel solution: Experimental and theoretical approaches. *Chem. Data Collect.* **2022**, *40*, 100870. [CrossRef]
22. Othman, N.H.; Ismail, M.C.; Mustapha, M.; Sallih, N.; Kee, K.E.; Jaal, R.A. Graphene-based polymer nanocomposites as barrier coatings for corrosion protection. *Prog. Org. Coat.* **2019**, *135*, 82–99. [CrossRef]
23. Chauhan, D.S.; Quraishi, M.A.; Ansari, K.R.; Saleh, T.A. Graphene and graphene oxide as new class of materials for corrosion control and protection: Present status and future scenario. *Prog. Org. Coat.* **2020**, *147*, 105741. [CrossRef]
24. Parthipan, P.; Cheng, L.; Rajasekar, A. *Glycyrrhiza glabra* extract as an eco-friendly inhibitor for microbiologically influenced corrosion of API 5LX carbon steel in oil well produced water environments. *J. Mol. Liq.* **2021**, *333*, 115952. [CrossRef]
25. Kumar, D.; Jain, V.; Rai, B. Imidazole derivatives as corrosion inhibitors for copper: A DFT and reactive force field study. *Corros. Sci.* **2020**, *171*, 108724. [CrossRef]
26. Feliu, S., Jr. Electrochemical impedance spectroscopy for the measurement of the corrosion rate of magnesium alloys: Brief review and challenges. *Metals* **2020**, *10*, 775. [CrossRef]
27. Arora, P.K.; Shrivastava, Y.; Kumar, H. Optimising FDM printing parameters for improved tensile properties in 3D printed ASTM D638 standard samples. *Aust. J. Mech. Eng.* **2023**, *23*, 277–290. [CrossRef]
28. Smith, G.M.; Gildersleeve, E.J.; Luo, X.T.; Luzin, V.; Sampath, S. On the surface and system performance of thermally sprayed carbide coatings produced under controlled residual stresses. *Surf. Coat. Technol.* **2020**, *387*, 125536. [CrossRef]
29. Nazarlou, Z.; Hosseini, S.F.; Seyed Dorraji, M.S.; Rasoulifard, M.H.; Aydemir, U. Ti_3C_2 MXene/polyaniline/montmorillonite nanostructures toward solvent-free powder coatings with enhanced corrosion resistance and mechanical properties. *ACS Appl. Nano Mater.* **2023**, *6*, 8804–8818. [CrossRef]
30. *ASTM D638-14*; Standard Test Method for Tensile Properties of Plastics. ASTM: West Conshohocken, PA, USA, 2015.
31. Hong, M.S.; Park, Y.; Kim, J.G.; Kim, K. Effect of incorporating MoS_2 in organic coatings on the corrosion resistance of 316L stainless steel in a 3.5% NaCl solution. *Coatings* **2019**, *9*, 45. [CrossRef]
32. Zhang, H.; Huang, X.; Tao, J.; Chen, X.; Yang, L. Corrosion resistance and mechanical properties of coating/steel substrate system in acid rain environment. *J. Constr. Steel Res.* **2023**, *201*, 107740. [CrossRef]
33. Almufarij, R.S.; El Sayed, H.A.F.; Mohamed, M.E. Eco-friendly approach for the construction of superhydrophobic coating on stainless steel metal based on biological metal–organic framework and its corrosion resistance performance. *Materials* **2023**, *16*, 4728. [CrossRef]

34. Samad, U.A.; Alam, M.A.; Abdo, H.S.; Anis, A.; Al-Zahrani, S.M. Synergistic effect of nanoparticles: Enhanced mechanical and corrosion protection properties of epoxy coatings incorporated with SiO_2 and ZrO_2. *Polymers* **2023**, *15*, 3100. [CrossRef]
35. Muresan, L.M. Nanocomposite coatings for anti-corrosion properties of metallic substrates. *Materials* **2023**, *16*, 5092. [CrossRef]
36. Abdelfattah, K.B.; Abbas, M.A.; El-Garaihy, W.H.; Mohamed, A.M.A.; Salem, H.G. Corrosion and degradation behavior of MCSTE-Processed AZ31 magnesium alloy. *Sci. Rep.* **2025**, *15*, 4072. [CrossRef]

Disclaimer/Publisher's Note: The statements, opinions and data contained in all publications are solely those of the individual author(s) and contributor(s) and not of MDPI and/or the editor(s). MDPI and/or the editor(s) disclaim responsibility for any injury to people or property resulting from any ideas, methods, instructions or products referred to in the content.